

## Supporting Information

### Influence of the hydrogen-bond interactions on the excited-state dynamics of a push-pull azobenzene dye: the case of Methyl Orange.

Christoph Nançoz,<sup>a</sup> Giuseppe Licari,<sup>a</sup> Joseph S. Beckwith,<sup>a</sup> Magnus Soederberg,<sup>a</sup> Bogdan Dereka,<sup>a</sup> Arnulf Rosspeintner,<sup>a</sup> Oleksandr Yushchenko,<sup>a</sup> Romain Letrun,<sup>a‡</sup> Sabine Richert,<sup>a¶</sup> Bernhard Lang,<sup>a</sup> and Eric Vauthey\*<sup>a</sup>

#### 1 Quantum-chemical calculations

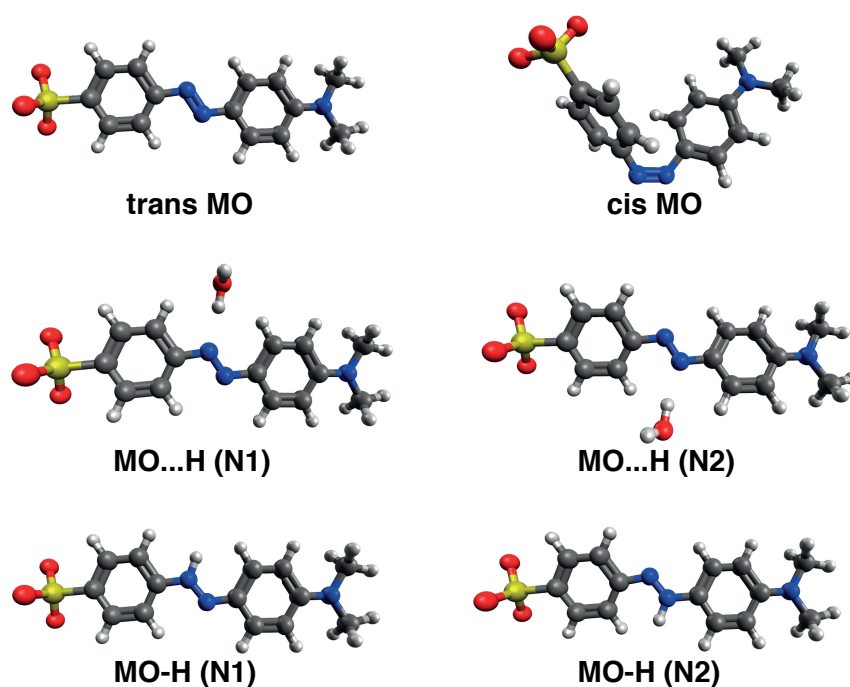


Fig. S1: Optimised structures of MO in different forms (trans or cis), in the trans form with an H-bonded water molecule, and in the protonated trans forms. All calculations were performed in water (PCM). See also Table 1 (main text).

<sup>a</sup> Department of Physical Chemistry, University of Geneva, 30 Quai Ernest-Ansermet, CH-1211 Geneva 4, Switzerland. E-mail: eric.vauthey@unige.ch

<sup>‡</sup> Present address: European XFEL GmbH, Holzkoppel 4, 22869 Schenefeld, Germany.

<sup>¶</sup> Present address: Centre for Advanced Electron Spin Resonance (CAESR), University of Oxford, South Parks Road, Oxford, OX1 3QR, U.K.

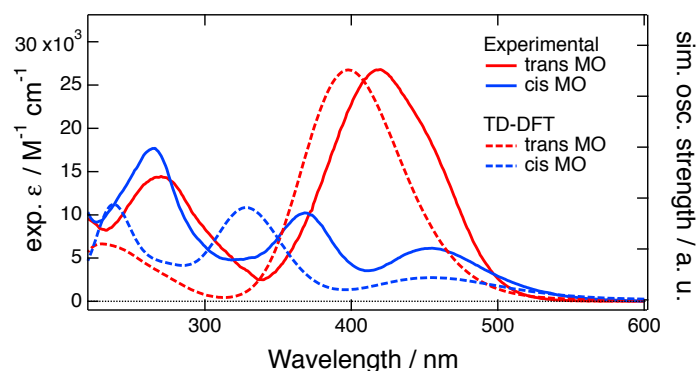


Fig. S2: Comparison between the experimental (in ACN) and calculated (TD-DFT, in water) electronic absorption spectra of MO in the trans and cis forms. The bandshapes were obtained by convolving the calculated intensities with a Gaussian function with 0.3 eV full-width at half-maximum. The experimental absorption spectrum of the cis form has been obtained from the results of the continuous illumination experiments (see Figure 8 main text).

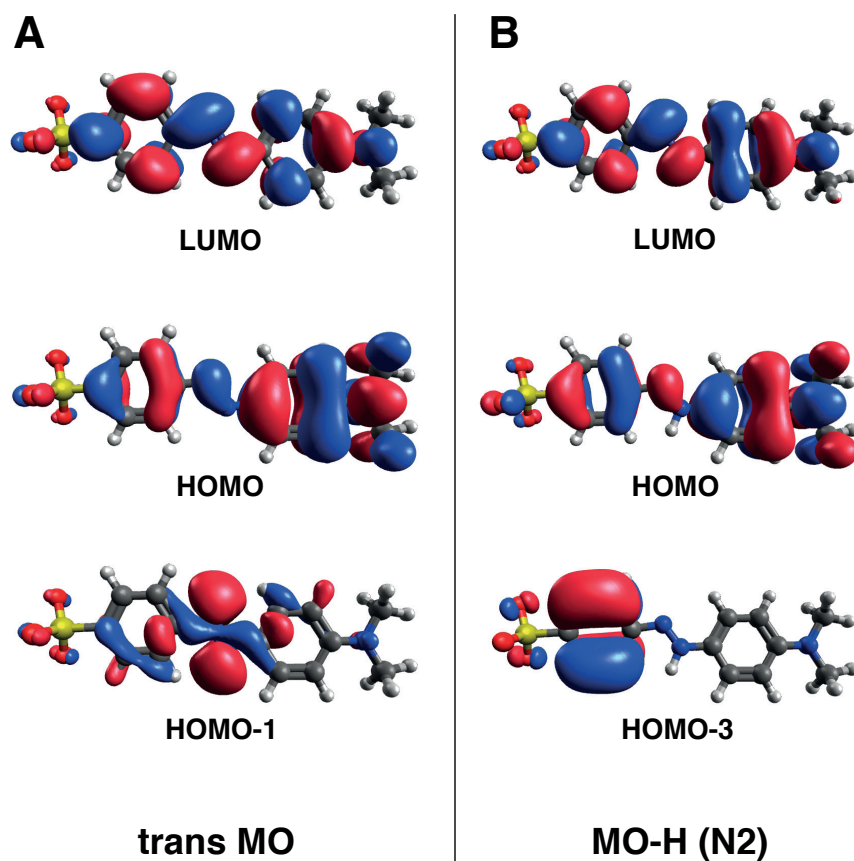


Fig. S3: Frontier molecular orbitals of (A) trans MO and (B) protonated MO at N2 (see Table ??, main text). In A, HOMO-1  $\rightarrow$  LUMO is the main contribution (90%) to the first excited state ( $n\pi^*$ ), whereas HOMO  $\rightarrow$  LUMO is the main contribution (93%) to the second excited state ( $\pi\pi^*$ ). In B, HOMO  $\rightarrow$  LUMO is the main contribution (96%) to the first excited state ( $\pi\pi^*$ ), whereas HOMO-3  $\rightarrow$  LUMO is the main contribution (93%) to the second excited state ( $\pi\pi^*$ ). The molecular orbitals were calculated at 0.02 isovalue.

## 2 Time-resolved fluorescence

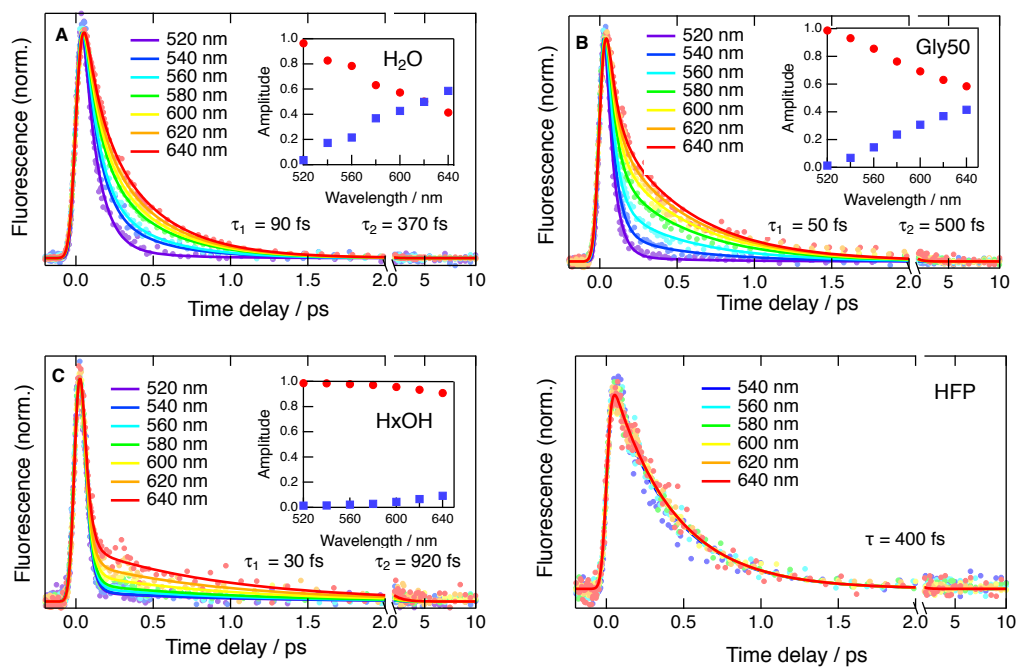


Fig. S4: Time profiles of the fluorescence of MO in water, water/glycerol (50%), hexanol and HFP at several wavelengths measured by fluorescence up-conversion upon 400 nm excitation and best fits obtained from global analysis using a biexponential (single exponential for HFP) function convolved with the instrument response function. Inset: relative amplitudes associated with the fast ( $A_1$ , red) and slow ( $A_2$ , blue) decay components.

### 3 Transient electronic absorption

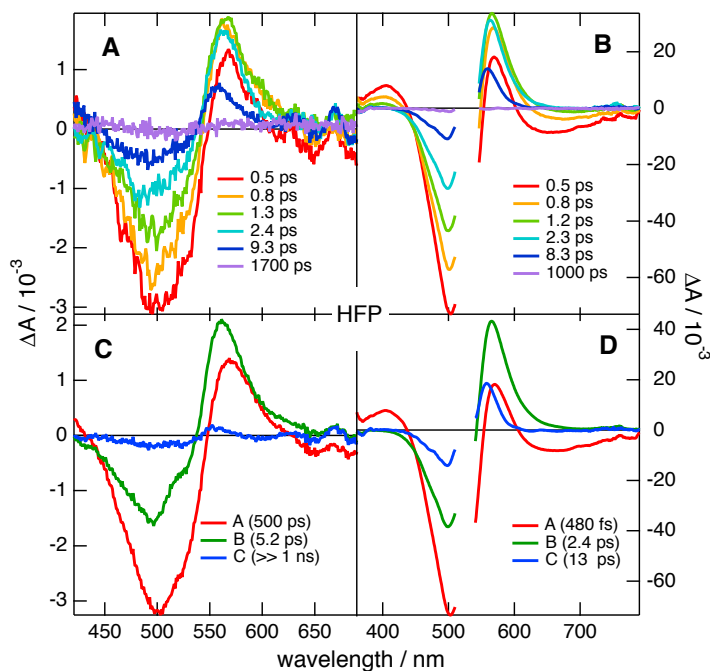


Fig. S5: (A,B) Transient electronic absorption spectra recorded at various time delays after (A) 400 nm or (B) 530 nm excitation of MO in HFP and (C,D) evolution-associated difference absorption spectra obtained from global analysis assuming three successive exponential steps,  $A \rightarrow B \rightarrow C \rightarrow$ .

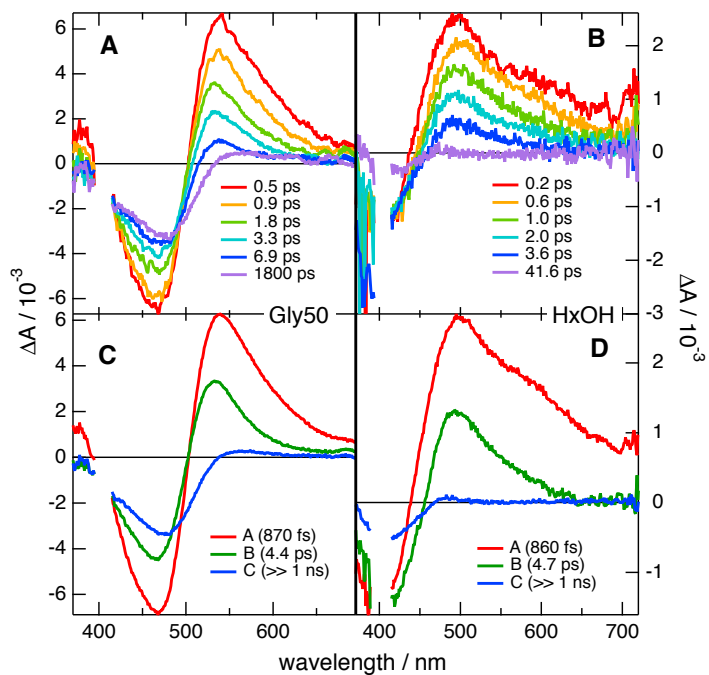


Fig. S6: (A,B) Transient electronic absorption spectra recorded at various time delays after 400 nm excitation of MO in (A) 50% (v/v) glycerol/water and (B) HxOH, and (C,D) evolution-associated difference absorption spectra obtained from global analysis assuming three successive exponential steps,  $A \rightarrow B \rightarrow C \rightarrow$ .

## 4 Vibrational spectroscopy

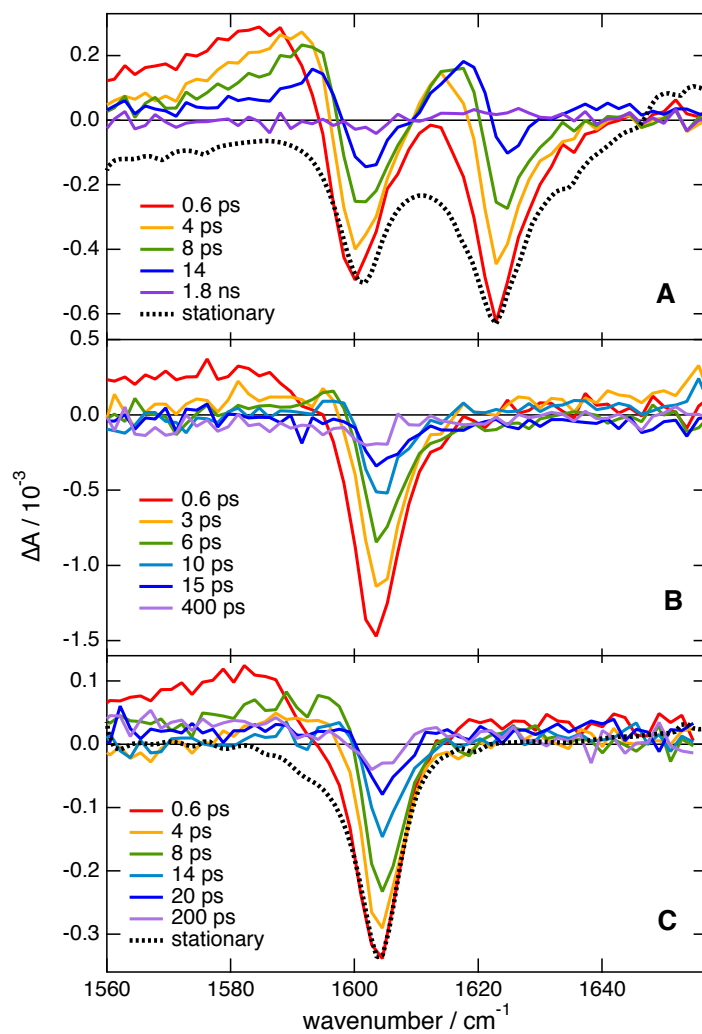


Fig. S7: Transient vibrational absorption spectra recorded at various time delays after 400 nm excitation of MO in (A) HFP, (B)  $\text{D}_2\text{O}$  and (C) MeOD. The inverse of the stationary IR absorption spectra of MO in the same solvents (Figure S8) are shown for comparison.

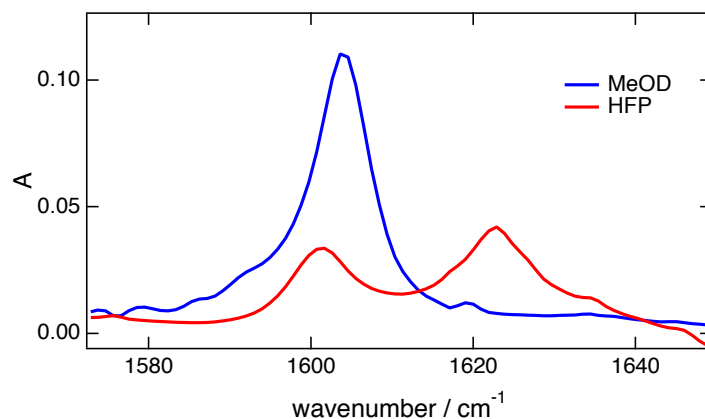


Fig. S8: Stationary IR absorption spectra of MO in MeOD and HFP. Because of the presence of strong solvent bands in this region, good stationary spectra of MO could not be recorded in  $D_2O$  and  $ACN_{d3}$ .

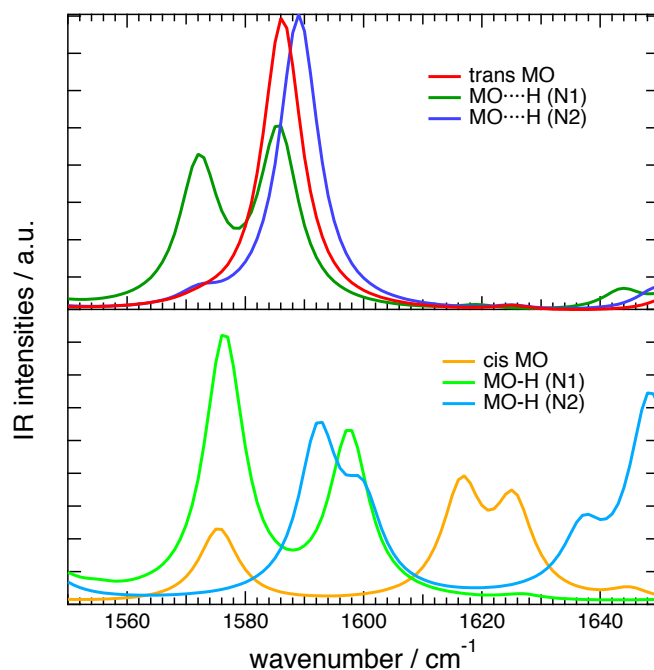


Fig. S9: Calculated IR absorption spectra (without frequency scaling) of MO in the different forms shown in Figure S1. All calculations were performed in water (PCM). The lineshapes were obtained by convolving the calculated intensities with a Lorentzian function with a  $4\text{ cm}^{-1}$  half-width at half-maximum.

## 5 Measurements upon continuous illumination

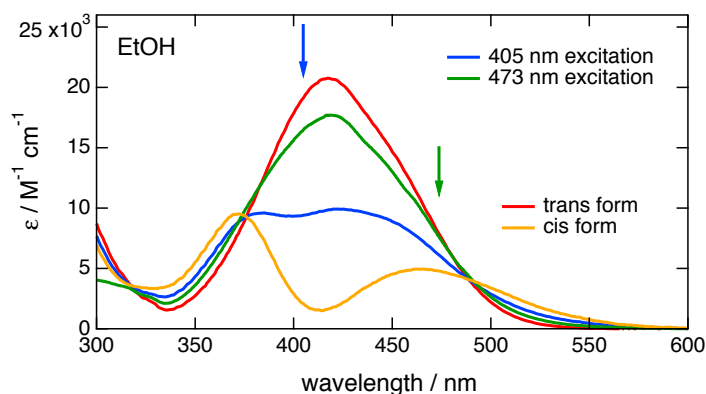


Fig. S10: Stationary electronic absorption spectra of MO in EtOH measured at photoequilibrium upon 405 or 473 nm illumination of MO in the trans form, and of MO in the cis form calculated using the Fischer method.<sup>1</sup> The vertical arrows represent the excitation wavelengths.

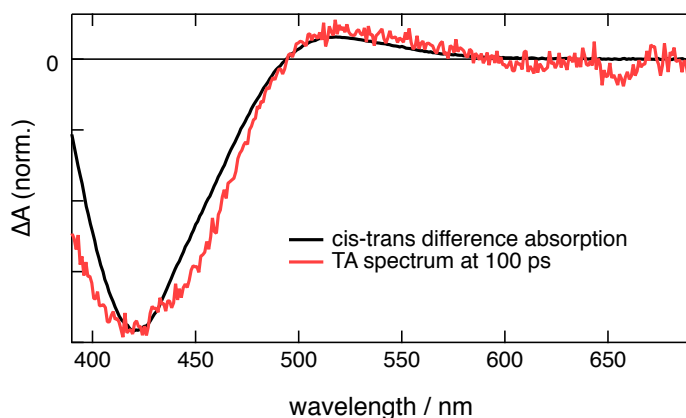


Fig. S11: Difference absorption spectrum of MO in the cis and trans forms in EtOH and transient absorption spectrum recorded 100 ps after 400 nm excitation of MO in EtOH.

The decay of the sample absorbance as a function of the irradiation time was analysed using the procedure described in ref.<sup>2</sup>(Figure ??A). Assuming that only the trans form is present before illumination starts, the time dependence of the trans-form concentration,  $C_t$ , upon irradiation is given by:<sup>2</sup>

$$\frac{dC_t}{dt} = \frac{I}{N_A V} [\phi_{ct}\beta_c(t) - \phi_{tc}\beta_t(t)] + k_{t,c \rightarrow t} C_c \quad (\text{S1})$$

where  $I$  is the photon flux in  $\text{s}^{-1}$ ,  $N_A$  the Avogadro number,  $V$  the sample volume in  $\text{dm}^3$ ,  $\phi_{tc}$  and  $\phi_{ct}$  the quantum yields of trans-to-cis and cis-to-trans isomerisation, respectively,  $\beta_t$  and  $\beta_c$  the fraction of light absorbed by each form, and  $k_{t,ct}$  the rate constant of the thermal cis-to-trans isomerisation. The latter can be directly obtained from the recovery dynamics of the absorbance after interrupting irradiation (Figure 9B). Knowing the absorption coefficients of both forms, and the photon flux,  $\phi_t$  and  $\phi_c$  can be obtained from a fit of eq(S1) to the measured decay of the absorbance upon illumination.<sup>2</sup> These best fits in EtOH and ACN are shown in (Figure 9A, main text) and the associated parameters are listed in Table S1.

Table S1: Isomerisation quantum yields obtained from the fit of eq.(S1) to the measured decay of the absorbance of MO at 420 nm (Figure 9A, main text) in two solvents and rate constants of thermal cis-to-trans isomerisation obtained from a single exponential fit of the absorption recovery after interrupting irradiation (Figure 9B).

Solvent	$\phi_{tc}$	$\phi_{ct}$	$k_{t,ct}$
ACN	0.07	0.18	$(120\text{s})^{-1}$
EtOH	0.14	0.94	$(24\text{s})^{-1}$

## References

- 1 E. Fischer, *J. Phys. Chem.*, 1967, **71**, 3704–3706.
- 2 K. Stranius and K. Börjesson, *Sci. Rep.*, 2017, **7**, 41145.